A Novel Design to Compensate Dispersion for Square-lattice Photonic Crystal Fiber over E to L Wavelength Bands

Shahram. Mohammad Nejad* and Nasrin. Ehteshami*
*Nanoptronics Research Center
School of Electrical Engineering, Iran University of Science and Technology, Tehran, Iran
Shahramm@iust.ac.ir , Ehteshami2010@hotmail.com

***Abstract*—This paper reveals a novel square-lattice photonic crystal fiber for dispersion compensation in a wide range of wavelengths. The 2-D finite difference frequency domain method (FDFD) with perfectly matched layers (PML) is used to investigate dispersion properties. It has been shown theoretically that it is possible to obtain high negative dispersion coefficient and confinement losses less than 10^{-5} dB/m in the entire wavelengths band.**

***Keyword*—chromatic dispersion, dispersion compensation fiber, square-lattice PCF, confinement loss.**

I. INTRODUCTION

The rapid development of the optical network and the increase in transmission rates imposes serious restrictions for residual chromatic dispersion in optical links. One of the best approach to minimize the penalty of chromatic dispersion for a large bandwidth of wavelengths is to use dispersion compensating fibers (DCF) [1]. The negative dispersion coefficient of conventional fiber is about D = -100 (ps/nm.km) at 1550nm wavelength with high losses [2]. This limitation in dispersion is mainly due to practical reasons such as material stress between the doped core and cladding regions, doping level, nonlinearity, as well as coupling losses. On the other hand, photonic crystal fibers (PCFs), a pure silica optical fibers with tiny air holes embedded in the host silica matrix running along the propagation axis, have attracted considerable attention from the optical scientific community [3]. One of the appealing properties of PCFs is the fact that they can possess dispersion properties significantly different than those of the conventional optical fibers. A desirable property of PCFs is that, the additional design parameters of air hole diameter d and holes pitch Λ offer much greater flexibility in the design of dispersion to get the required application. By manipulating air hole diameter d and pitch Λ, in PCFs facilitate a complete control on its properties, such as negative dispersion. Several designs of dispersion compensating PCFs (DCPCFs) have been reported in the international literatures [4]. Typically, the air holes are arranged on the vertex of an equilateral triangle with six air holes in the first ring surrounding the core, this type is called the hexagonal PCF (H-PCF) or conventional PCF. Besides the hexagonal structures, other design structures such as square-lattice, honeycomb and octagonal-lattice have been proposed for the PCF. But still, the demand for a simple dispersion compensation PCF structure exists in order to realize high negative dispersion and low confinement loss. Previous designs are all based on triangular PCFs, and report on negative dispersion properties of square-lattice PCFs over E to L wavelength bands is very few [5].

Various DCFs that were optimized to compensate for the dispersion in a single band, e.g., the S-band (1460-1530 nm), C-band (1530-1565 nm), and L-band (1565-1625nm), have been reported [6]. However, it is difficult for the DCF to compensate for dispersion over lower band, i.e. the E-band (1360-1460nm).

In this paper, we propose a new kind of square-lattice PCF with five rings air holes for dispersion compensation over E to L wavelength bands. The designed square-lattice PCF is based on dual concentric core refractive index profile, where the fiber supports two cores, namely central core and ring-core. The optical field transits to the ring-core after a particular wavelength [7]. We will investigate the loss and dispersion characteristics of the designed PCFs over E to L wavelength bands. There are three degrees of freedom; air holes diameter of the first ring, air holes diameter of second ring around the core and pitch of the lattice; those three parameters are adjusted separately and their influence on the dispersion curve is investigated. The calculated results show that our proposed PCF can simultaneously realize negative dispersion and low confinement losses in a wide wavelength range. This paper is organized as follows: In the next section, the theory of FDFD is described. In section III, it is focused on the PCF characteristics. In section IV, fiber geometry structure has been shown Finally, numerical results are discussed in section V.

II. ANALYSIS METHOD

The finite difference frequency domain (FDFD) is popular and appealing for numerical electromagnetic simulation due to its many merits. It has been one of the major tools for the analysis and understanding of PCFs. The discretization scheme can be derived from the Helmholtz equations or Maxwell's equations directly. Now we use the direct discretization schemes first described for photonic crystal fibers by Zhu et al [8]. Now we use the direct discretization schemes described for photonic crystal fibers. Yee's two-dimensional mesh is illustrated in Fig. 1; note that the transverse fields are tangential to the unit cell boundaries, so the continuity conditions are automatically satisfied. After inserting the equivalent nonsplit-field anisotropic PML in the

978-1-86135-370-2/10

frequency domain, the curl Maxwell equations are expressed as:

$$jk_0 s\varepsilon_r E = \nabla \times H \qquad (1)$$
$$-jk_0 s\mu_r H = \nabla \times E$$

$$s = \begin{bmatrix} s_y/s_x & 0 & 0 \\ 0 & s_x/s_y & 0 \\ 0 & 0 & s_x s_y \end{bmatrix} \qquad (2)$$

where μ_r and ε_r are the relative permittivity and permeability of the medium considered, $k_0 = 2\pi/\lambda$ is the wave number in free space, $s_x = 1 - \sigma_x / j\omega\varepsilon_0$, $s_y = 1 - \sigma_y / j\omega\varepsilon_0$ and σ is the conductivity profile. Assuming that the PCFs are lossless and uniform and the propagation constant along the z direction is β. Thus, the field variation along the propagation direction z is of the form $\exp(-j\beta z)$. The z-derivatives, $\partial/\partial z$, can be replaced by $-j\beta$ in Maxwell's equations and thus three dimensional equations can be solved using only a two dimensional mesh. Using the central difference scheme and zero boundary conditions outside of the anisotropic PML layers, the curl equations (1) can be rewritten in a matrix form which includes six field components. Then eliminating the longitudinal magnetic and electric fields, the eigenvalue matrix equation in terms of transverse magnetic fields and transverse electric fields can be obtained as:

$$\begin{bmatrix} Q_{xx} & Q_{xy} \\ Q_{yx} & Q_{yy} \end{bmatrix} \begin{bmatrix} H_x \\ H_y \end{bmatrix} = \beta^2 \begin{bmatrix} H_x \\ H_y \end{bmatrix} \qquad (3)$$

$$\begin{bmatrix} P_{xx} & P_{xy} \\ P_{yx} & P_{yy} \end{bmatrix} \begin{bmatrix} E_x \\ E_y \end{bmatrix} = \beta^2 \begin{bmatrix} E_x \\ E_y \end{bmatrix} \qquad (4)$$

Where the Q and P are highly sparse coefficient matrices. The order and the nonzero elements in them are reduced and effectively stored in sparse format, so the computation efficiency is improved greatly. The complex propagation constant β and the transversal magnetic or electric field distribution can be solved out quickly and accurately by a sparse matrix solver [9].

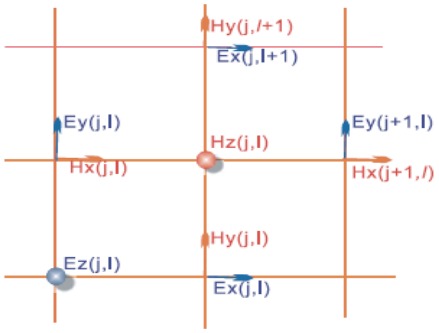

Figure 1. Unit cell in Yee's 2D-FDFD mesh

III. PHOTONIC CRYSTAL FIBER CHARACTERISTICS

A. Chromatic Dispersion

The chromatic dispersion D of a PCFs is easily calculated from the n_{eff} value vs. the wavelength using the following [2]:

$$D(\lambda) = -\frac{\lambda}{c}\frac{d^2\,\mathrm{Re}[n_{eff}]}{d\lambda^2} \qquad (5)$$

in (ps/(nm.km)), where Re(n_{eff}) is the real part of the refractive index, λ is the operating wavelength, and c is the velocity of light in a vacuum. The material dispersion can be obtained from the three-term sellmeier formula and is directly included in the calculation. In PCFs, the chromatic dispersion D is related to the additional design parameters like geometry of the air holes, pitch, and hole diameters. By optimizing these parameters, suitable guiding properties can be obtained.

B. Confinement Loss

Confinement loss is the light confinement ability within the core region. The increase of air hole rings help the confinement of light in the core region, which results in smaller losses than those with less air hole rings. Also, increasing the air holes diameter results in the increasing of the air filling fraction and consequently decreasing the loss. The confinement loss L_c is then obtained from the imaginary part of n_{eff} as follows [2]:

$$L_c = \frac{(20\times10^6)}{\ln(10)} k_0\,\mathrm{Im}[n_{eff}] \qquad (6)$$

With the unit dB/m, where Im (n_{eff}) is the imaginary part of the refractive index, $k_0 = 2\pi/\lambda$ is the wave number in the free space.

IV. DESIGN MODEL

The proposed PCF is made of pure silica and has a square array of air holes running along its length. This is an index guiding PCF. The transverse cross-section of the PCF is shown in Fig. 2, where Λ is the pitch of the lattice, d_1 is the air hole diameter of first ring, d_2 is the air-hole diameter of second ring and d is the air hole diameter in other rings. The air holes of the first ring are relatively large, since it is known that an increase in the air hole diameter of the first ring causes the dispersion coefficient to decrease. The air holes of the second ring are relatively smaller, because a ring of reduced diameter induces a change in the slope of the evolution of the effective index versus wavelength [7]. The total number of air hole rings was chosen to be five in order to simplify as much as possible the structural composition of the PCF. Fig.3 and Fig.4 show the effective index profile over E to L wavelength bands and the mode field distribution of the PCF at wavelength of 1550nm. The mode field distribution has its maximum amplitude at the center core region. Since the mode field of the PCF is largely inside the inner core, the dispersion characteristic of the PCF is more sensitive to the inner core structure. The design process of PCF requires the following steps. The essential geometric parameters of the PCF configuration, included

shape and size of the air-holes, the number of air-hole rings and background material are chosen in the first step. Then mode analysis refers to evaluation of the PCF guided modes and selecting a well confined mode is performed in the next step. The square-lattice PCF characteristics of the selected mode; e.g. effective index, dispersion, and loss are calculated in frequency analysis [10].

V. NUMERICAL RESULT AND DISCUSSION

The square-lattice PCF employs three different parameters to produce relatively high negative dispersion in a wide wavelength range. The dispersion curve of the designed PCF with $d=1.35\mu m$, $d_1=0.8\mu m$, $d_2=0.45\mu m$, and $\Lambda=1.36\mu m$ from E to L band is shown in Fig. 5. As it can be seen, the designed square-lattice PCF has negative dispersion of -100.4 ~ -130.32 (ps/nm.km) over E-band. In addition , the PCF shows negative dispersion of -130.3 ~ -138(ps/nm.km), -137.8 ~ -138.1 (ps/nm.km), -138.1 ~ -134 (ps/nm.km) over S, C and L bands respectively.

Table I, II, and III summarize the dispersion variation in the square-lattice PCF with altering the hole diameters of the inner two rings and pitch of the lattice ; d_1, d_2, and Λ respectively. With respect to Tables I, II, and III, the lowest negative dispersion variation is achieved in the C band for square-lattice PCF with the following parameters; $d=1.35\mu m$, $d_1=0.8\mu m$, $d_2=0.45\mu m$, and $\Lambda=1.36\mu m$. It has ultra-flattened negative dispersion with slop=0.00857 (ps/nm^2/km) over C band.

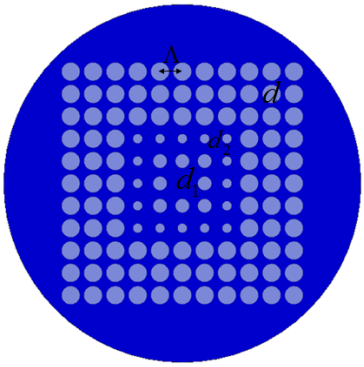

Figure 2. Cross section of square-lattice PCF

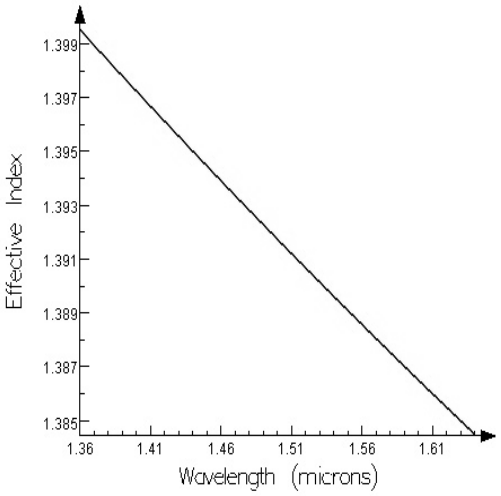

Figure 3. Effective index curve of the PCF as a function of wavelength. $d=1.35\mu m$, $d_1=0.8\mu m$, $d_2=0.45\mu m$, and $\Lambda=1.36\mu m$.

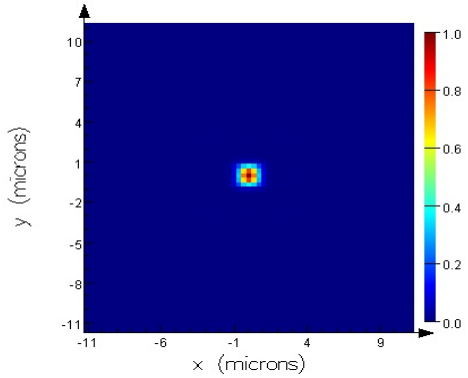

Figure 4. Transversal field intensity distribution at a wavelength of $\lambda=1550nm$ for the fundamental guiding mode. $d=1.35\mu m$, $d_1=0.8\mu m$, $d_2=0.45\mu m$, and $\Lambda=1.36\mu m$

So, dispersion is more sensitive to the inner hole diameter; d_1 that play important role in the inner core structure. From Table I, it can be seen that the absolute values of the negative dispersion coefficient increase considerably as d_1 increase. Also, d_2 is the important parameter of the square-lattice PCF to achieve negative dispersion over a wide wavelength range. From Table II, it is found that by decreasing d_2, larger negative dispersion coefficient and better dispersion slope compensation are possible. From Table III, it is clearly seen that the parameter Λ dominantly influences the dispersion level (the dispersion increases as Λ increases), but it has little effect on the dispersion flatness. The rings with air hole diameters of d is as farther from central core, it does not have significant effect on dispersion.

The loss characteristics of square-lattice PCF with $d=1.35\mu m$, $d_1=0.8\mu m$, $d_2=0.45\mu m$, and $\Lambda=1.36\mu m$, within the wavelength range of 1360-1630 nm is shown in Fig. 6. With respect of Fig. 6, the loss of the designed square-lattice PCF is 0.00(dB/km) over E-band. In addition, the square-lattice PCF shows the losses of 0.00~ 0.25×10^{-3} (dB/km), 0.25×10^{-3} ~ 0.54×10^{-3} (dB/km), 0.54×10^{-3} ~ 1.68×10^{-3} (dB/km) over S, C, and L bands respectively. Tables IV, V, and VI summarize the losses of the square-lattice PCF with altering the hole diameters; d_1, d_2 and pitch of the lattice Λ respectively, at wavelength of 1550nm.

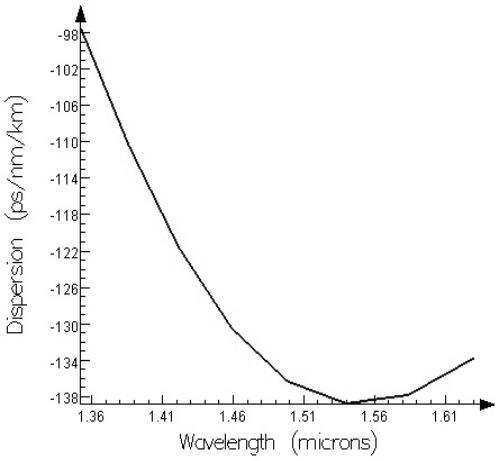

Figure 5. Dispersion curve of the PCF as a function of wavelength. $d=1.35\mu m$, $d_1=0.8\mu m$, $d_2=0.45\mu m$, and $\Lambda=1.36\mu m$

TABLE I.
DISPERSION OF THE SQUARE-LATTICE PCF WITH DIFFERENT d_1 OVER E-BAND TO L-BAND, $d = 1.35\mu m$, $d_2 = 0.45\mu m$, and $\Lambda = 1.36\mu m$

d_1 (μm)	Dispersion (ps/nm/km) E-band	Dispersion (ps/nm/km) S-band	Dispersion (ps/nm/km) C-band	Dispersion (ps/nm/km) L-band
0.8	-100.4 ~ -130.2	-130.3 ~ -138	-137.8 ~ -138.1	-138.1 ~ -134
0.84	-109.08~ -147.5	-147.5 ~ -156.6	-156.7 ~ -156.3	-156.3 ~ -150.09
0.88	-139.7~ -182.9	-182.9 ~ -183.2	-183.2 ~ -178	-178 ~ -161
0.92	-160.9~ -213.6	-213.7 ~ -205.5	-205.5 ~ -193.1	-193.1 ~ -169.5

TABLE II.
DISPERSION OF THE SQUARE-LATTICE PCF WITH DIFFERENT d_2 OVER E-BAND TO L-BAND, $d = 1.35\mu m$, $d_1 = 0.92\mu m$, and $\Lambda = 1.36\mu m$

d_2 (μm)	Dispersion (ps/nm/km) E-band	Dispersion (ps/nm/km) S-band	Dispersion (ps/nm/km) C-band	Dispersion (ps/nm/km) L-band
0.45	-160.9~ -213.6	-213.7 ~ -205.5	-205.6~ -193.1	-193.1~ -169.5
0.5	-64.6~ -143.1	-143.12~ -190.9	-191~ -207.3	-207.3~ -221.5
0.55	-17.84~ -74.4	-74.5~ -121.1	-121.2~ -144.1	-144.1~ -180.02
0.6	4.44~ -37.44	-37.44~ -74.3	-74.4~ -94	-94~ -128/9

TABLE III.
DISPERSION OF THE SQUARE-LATTICE PCF WITH DIFFERENT Λ OVER E-BAND TO L-BAND, $d = 1.35\mu m$, $d_1 = 0.92\mu m$, and $d_2 = 0.45\mu m$

Λ (μm)	Dispersion (ps/nm/km) E-band	Dispersion (ps/nm/km) S-band	Dispersion (ps/nm/km) C-band	Dispersion (ps/nm/km) L-band
1.36	-160.9~ -213.6	-213.7~ -205.5	-205.6~ -193.1	-193.1~ -169.5
1.38	-169.4~ -209.88	-209.88~ -192.63	-192.63~ -177.6	-177.6~ -153.24
1.4	-141.3~ -199.6	-199.6 ~ -195.6	-195.6~ -184	-184~ -159.9
1.6	-97.88~ -96.62	-96.62~ -82.5	-82.6~ -75.22	-75.22~ -63.5

As Table IV shows, the loss increases with increasing the hole diameter of the inner ring; d_1. It is due to the increment of the effective core area by increasing d_1. On the other hand, the loss decreases with increment of d_2. (see Table V).

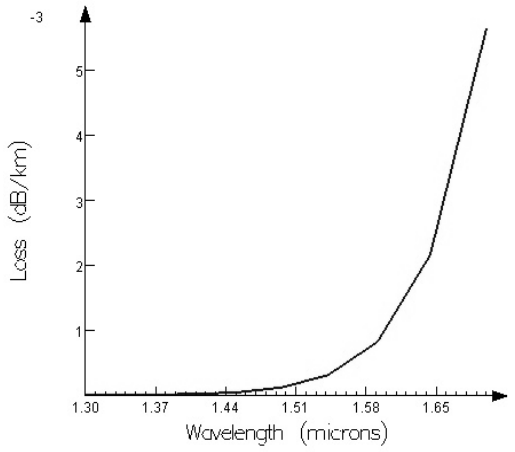

Figure 6. Loss curve of the PCF as a function of wavelength. $d = 1.35\mu m$, $d_1 = 0.8\mu m$, $d_2 = 0.45\mu m$, and $\Lambda = 1.36\mu m$

It can be explained by the air filling fraction parameter, increment of d_2 result in the increment of the air filling fraction, and consequently the decrement of the loss. From Table VI, it is found that loss is increased with increasing pitch when other parameters are remained same. The loss remains below $10^{-5} dB/m$ from $1.36\mu m$ to $1.63\mu m$ wavelength for choosing five air hole rings.

In order to see the difference with different geometry structures, we compare dispersion between square-lattice PCF and triangular one with the same structure. From Table VII, we can see that the difference of dispersion between these two types of PCFs is not high, especially at long wavelength. Moreover, the dispersion value obtained with square-lattice PCF is between – 160.9 and -169.5 (ps/nm.km) with corresponding wavelength from $1.36\mu m$ to $1.63\mu m$, while -81.2 and -235.7 (ps/nm.km) for triangular one in this range. This indicate that proposed square-lattice PCF can achieve better dispersion compensation with lower slope than triangular one over C-band.

TABLE IV.
LOSS OF THE SQUARE-LATTICE PCF WITH DIFFERENT d_1 AT A WAVELENGTH OF $\lambda = 1550nm$. $d = 1.35\mu m$, $d_2 = 0.45\mu m$, and $\Lambda = 1.36\mu m$

d_1 (μm)	Loss (dB/km)
0.8	0.361×10^{-3}
0.84	0.505×10^{-3}
0.88	0.866×10^{-3}
0.92	1.27×10^{-3}

TABLE V.
LOSS OF THE SQUARE-LATTICE PCF WITH DIFFERENT d_2 AT A WAVELENGTH OF $\lambda = 1550nm$. $d = 1.35\mu m$, $d_1 = 0.92\mu m$, and $\Lambda = 1.36\mu m$

d_2 (μm)	Loss (dB/km)
0.45	1.27×10^{-3}
0.5	0.621×10^{-3}
0.55	0.261×10^{-3}
0.6	0.124×10^{-3}

TABLE VI.
LOSS OF THE SQUARE-LATTICE PCF WITH DIFFERENT Λ AT A WAVELENGTH OF $\lambda = 1550nm$. $d = 1.35\mu m$, $d_2 = 0.45\mu m$, and $d_1 = 0.92\mu m$

Λ (μm)	Loss (dB/km)
1.36	0.127×10^{-2}
1.38	0.139×10^{-2}
1.4	0.155×10^{-2}
1.6	0.790×10^{-2}

VI. CONCLUSION

In this paper, a square-lattice PCF for dispersion compensation is proposed. From the numerical simulation results, it is found that it is possible to obtain larger negative dispersion, better dispersion slope, and low confinement loss in the entire E+S+C+L wavelength telecommunication bands. Another main advantage is that, compared with previously presented square-lattice PCFs, the design procedure for this proposed novel square-lattice PCF structure could be more efficient and easier because relatively fewer geometrical parameters are need to be optimized. Thus, we can choose the appropriate geometric parameters to achieve the desirable dispersion compensation over different communication bands. Take all things to account; we believe that our proposed PCF will be useful in dispersion compensation ultra-broadband transmission application.

TABLE VII.
DISPERSION OF THE SQUARE-LATTICE PCF AND TRIANGULAR LATTICE PCF OVER E-BAND TO L-BAND, $d = 1.35\mu m$, $d_1 = 0.92\mu m$, $d_2 = 0.45\mu m$, and $\Lambda = 1.36\mu m$

structure of PCF	Dispersion (ps/nm/km) E-band	Dispersion (ps/nm/km) S-band	Dispersion (ps/nm/km) C-band	Dispersion (ps/nm/km) L-band
Triangular lattice	-81.2 ~ -158.5	-158.5 ~ -202.7	-202.7 ~ -218.6	-218.6 ~ -235.7
Square lattice	-160.9 ~ -213.6	-213.7 ~ -205.5	-205.5 ~ -193.1	-193.1 ~ -169.5

REFERENCES

[1] K. Mukasa, T. Yagi, "Dispersion flat and low non-linear optical link with new type of reverse dispersion fiber (RDF-60)," Proc. TuH7-1, *Optical Fiber Communication Conference*, 2001.

[2] Feroza Begum, Yoshinori Namihira, S.M. Abdur Razzak, Shubi Kaijage, Nguyen HoangHai, Tatsuya Kinjo, Kazuya Miyagi, Nianyu Zou, "Novel broadband dispersion compensating photonic crystal fibers: Applications in high-speed transmission systems," *Optics & Laser Technology,* vol.41, pp. 679-686, 2009.

[3] S.K. Varshney, N.J. Florous, K. Saitoh, M. Koshiba, T. Fujisawa, " Numerical investigation and optimization of a photonic crystal fiber for simultaneous dispersion compensation over S+C+L wavelength bands," *Optics Communications*, vol 274, pp.74-79, 2007.

[4] Jingyuan Wanga, Chun Jianga, Weisheng Hua, Mingyi Gao, "Modified design of photonic crystal fibers with flattened dispersion," *Optics & Laser Technology*, vol.38, pp.169-172, 2006.

[5] TAN Xiao-ling, GENG You-fu, TIAN Zhen, WANG Peng, and YAO Jian-quan, "Study of ultra-flattened dispersion square-lattice photonic crystal fiber with low confinement loss," *Optoelectronics Lerrers*, vol.5, no.2, pp.0124-0127, 2007.

[6] L. Gruner-Nielsen, S. Knudsen, T. Veng, B. Edvold, and C. Larsen, "Design and manufacture of dispersion compensating fiber for simultaneous compensation of dispersion and dispersion slope," *Proceeding of .OFC*, San Diego, CA, pp.232-234, Mar.1999.

[7] Zinan Wang, Xiaomin Ren, Xia Zhang, Yongzhao Xu and Yongqing Huang, "Design of a microstructure fiber for slope-matched dispersion compensation," *J.Opt.A: Pure Appl.Opt*, vol.9, pp.435-440, 2007.

[8] Zhu Z. and Brown T. G., "Analysis of the fundamental space-filling mode of photonic crystal fibers: a symmetry point of view," *Opt. Express*, no.10, pp.853-864, 2002.

[9] M Pourmahyabadi and Sh. Mohammad Nejad, " Numerical analysis of Index-Guiding photonic crystal fibers with low confinement loss and ultra-flattened dispersion by FDFD method," *Journal of Electrical and Electronic Engineering Department of Electrical Engineering Iran University of Science & Technology,* vol. 5, no. 3, pp.170-179 , Sep. 2009.

[10] Sh. Mohammad Nejad, M. Aliramezani, M. Pourmahyabadi, "Design and simulation of a dual-core photonic crystal fiber for dispersion compensation over E to L wavelength band," *International Symposium on Telecommunications,* pp.138-43, 2008